SME Annual Meeting
Feb. 24 - 27, 2013, Denver, CO

Preprint 13-010

TRACE ELEMENTS IN PORPHYRY COPPER SYSTEMS AS STRATEGIC MINERALS

R. I. Yano, UNR, Reno, NV
J. G. Price, Nevada Bureau of Mines and Geology-UNR, Reno, NV
T. Thompson, UNR, Reno, NV
P. Emsbo, US Geological Survey, Denver, CO
A. Koenig, US Geological Survey, Denver, CO

ABSTRACT

Analyses of trace elements in bulk ores and in chalcopyrite and other ore minerals from porphyry copper systems worldwide, including skarns and breccia pipes, reveal some key factors regarding byproduct critical elements. Petrographic and scanning electron microscope analyses combined with a laser ablation inductively coupled plasma mass spectrometry technique developed by the USGS on selected ores from the Mackay-Stanford Ore Deposits Collection suggest that selenium occurs as atomic substitutions in sulfides, particularly pyrrhotite (up to 430 ppm) and chalcopyrite (up to 300 ppm Se); tellurium occurs predominantly as less-than-five-micron-sized inclusions of bismuth-tellurium minerals in other ore minerals, particularly chalcopyrite; cobalt and nickel are locally enriched in pyrite (up to 7800 ppm Co and 9100 ppm Ni); gallium is locally enriched in magnetite (up to 83 ppm Ga); indium and silver are locally enriched in chalcopyrite (up to 890 ppm In and 770 ppm Ag); cadmium substitutes for zinc, particularly in sphalerite (up to 4100 ppm Cd). There is considerable variation, both between and within individual deposits, in both selenium and tellurium content in these copper ores, ranging from 0.6 to 148 ppm Se and 0.09 to 64 ppm Te. Indium tends to be high in copper ores that are also enriched in silver. At current prices, many of these elements are sufficiently enriched to warrant investigation into metallurgical recovery as byproducts of the major elements.

INTRODUCTION

In recent years, there has been a growing interest in trace elements that, historically, have had little economic significance (cf. Eggert et al. 2008; Latiff et al. 2008; Jaffee et al. 2011). This increase in demand has largely been due to the development of new trace element-based technologies that underpin several green energy and defense applications. For example, thin-film photovoltaic technology for solar panels has opened markets forlow-priced cadmium, tellurium, and selenium. Batteries in electric cars require lithium. Wind turbines use rare earth-bearing magnets for generating electricity. Gas turbines use specialty alloys, including cobalt and rhenium. Gallium is widely used in electronics, including integrated circuits and light-emitting diodes. Indium has become critical for use in liquid crystal displays. There are no large-scale primary sources for many of these elements; many are byproducts of various other metals. For example, selenium and tellurium are byproducts of copper production, gallium is a byproduct of aluminum production, cadmium is a byproduct of zinc production, and indium is a byproduct of zinc, copper, and tin production.

METHODS

In this study, which is an extension of work by Yano (2012), we focus on the energy-critical elements that occur as potential byproducts in porphyry copper systems, including skarns and breccia pipes. Ore samples from the Mackay-Stanford Ore Deposits Collection at the University of Nevada, Reno were selected from a variety of porphyry copper systems (Table 1). The collection includes tens of thousands of samples collected by Stanford and Mackay professors, students, and donors from many classic ore deposits throughout the world. The samples were split with one split retained within the Mackay-Stanford collection for making polished thin sections and two splits sent to the U.S. Geological Survey project on "Quick Assessment of Rare and Critical Metals in Ore Deposits: A National Assessment," where one split was powdered for bulk-rock analysis and another split was preserved for follow-up trace-element analyses.

Table 1. List of samples analyzed in this study, with type of ore deposit and key references.

Sample #	Location	Deposit type
NC08-39	E2 orebody, Pumpkin Hollow, Lyon Co., Nevada[1]	skarn
NC08-49	East orebody, Pumpkin Hollow, Lyon Co., Nevada	skarn
NC08-20	North orebody, Pumpkin Hollow, Lyon Co., Nevada	skarn
NC08-19&25	South orebody, Pumpkin Hollow, Lyon Co., Nevada	skarn
MVHD	Mason Valley mine, Lyon Co., Nevada[2]	skarn
STSG	Minnesota (Standard Slag) mine, Douglas Co., Nevada[3]	skarn
OD13152	Fritz Island, Pennsylvania[4]	skarn
OD31730,	Outokumpu mine, Finland[5]	skarn
OD31756, &		
OD31759		
OD14895	Republic, Johnson Camp, Arizona[6]	skarn
OD20023	Elisa mine, Cananea, Sonora, Mexico[7]	skarn
OD20001,	La Colorado mine, Cananea, Sonora, Mexico[8]	breccia pipe
OD20003, &		
OD20104		
OD20021	Capote mine, Cananea, Sonora, Mexico[8]	breccia pipe
JP205-30&33	Victoria mine, Elko Co., Nevada[9]	breccia pipe
Yer-3,4,5,6 &	Yerington mine, Lyon Co., Nevada[10]	porphyry copper
OD10808		
JP205-2,5A,	Bingham Canyon, Salt Lake Co., Utah[11]	porphyry copper
5B &		
OD9927		
OD3673	Gardner mine, Bisbee, Arizona[12]	porphyry copper
OD43579	Mission, Arizona[13]	porphyry copper
OD16922	Bagdad, Arizona[14]	porphyry copper
OD47214 &	Chiquicamata mine, Chile[15]	porphyry copper
OD21422		
OD28536 &	El Teniente mine, Chile[16]	porphyry copper
OD28539		
Gras-1	Grasberg, Irian Jaya, Indonesia[17]	porphyry copper

[1]Einaudi (1977), Harris and Einaudi (1984), Dilles (1987)& Doebrich et al. (1996), [2]Moore (1969) & Einaudi (1977), [3]Moore (1969), [4]Spencer (1908), [5]Peltola (1978) & Loukola-Ruskeeniemi (1999), [6]Baker (1960), [7]Meinert (1982), [8]Meinert (1982) & Bushnell (1988), [9]LaPointe et al. (1992), [10]Proffett and Dilles (1984), Carten (1986), Dilles (1987), & Seedorff et al. (2008), [11]Lanier et al. (1978) & Redmond & Einaudi (2010), [12] Livingston et al. (1968) & Lowell and Guilbert (1970), [13] Livingston et al. (1968) & Lowell and Guilbert (1970), [14] Anderson (1950) & Livingston et al. (1968), [15]Ossandon et al. (2001), [16]Klemm et al. (2007), [17]Pollard et al. (2005).

The powdered samples were analyzed using the laser ablation inductively coupled plasma-mass spectrometry (LA-ICP-MS) technique developed by the U.S. Geological Survey (Emsbo et al. 2010) to determine the bulk rock geochemistry (Fig. 1). Samples with elevated concentrations of the trace elements of interest were selected for

follow-up petrography using both transmitted and reflected light. Selectedpolished thin sections were then taken to Denver, where detailed scanning electron microscope (SEM) and LA-ICP-MS analyses were conducted to determine the trace element residences and abundance by mineral phase using traditional LA-ICP-MS spot microanalysis (see Wilson et al. 2002). Concentrations for LA-ICP-MS spot analyses were calculated using the standard methods of Longerich et al. (1996).

Results of the LA-ICP-MS analyses of bulk ore samples are listed in Table 2, and results of LA-ICP-MS spot analyses of minerals are listed in Tables 3 (chalcopyrite), 4 (magnetite), 5 (pyrite), and 6 (pyrrhotite, bornite, chalcocite, tennantite, covellite, enargite, and sphalerite).Detection limits vary by mineral analyzed and by other operating conditions. The detection limits during the analyses in this study are listed in Table 7.

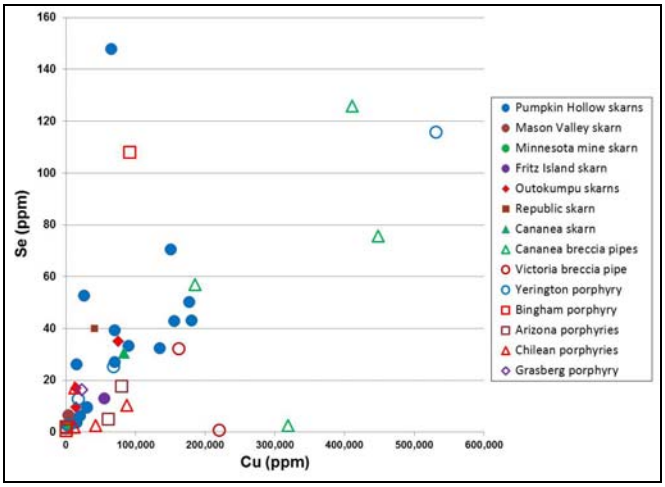

Figure 1. Plot of selenium versus copper in bulk-rock ore samples from porphyry copper systems.

OBSERVATIONS

Selenium and Cobalt in Chalcopyrite

Selenium is concentrated in most chalcopyrites (Fig. 2), and cobalt is locally concentrated in chalcopyrite in some deposits. In particular, the Outokumpu skarns (Fig. 3), which are associated with serpentinites, are understandably enriched in cobalt, an element that is typically more abundant in mafic rocks than in silicic rocks. The highest concentrations of selenium detected in chalcopyrites in this study are from the Pumpkin Hollow skarn (300 ppm), Grasberg porphyry (220 ppm), and Yerington porphyry (190 ppm). A pyrhhotite from Pumpkin Hollow contains the highest selenium concentration of any of the minerals analyzed in this study (430 ppm). Due to similarities in charge and size (1.84 Å for S^{2-} and 1.91 Å for Se^{2-}), and as documented by Sindeeva (1964), selenium is accommodated presumably as atomic substitutions for sulfur in solid solution in sulfide minerals.

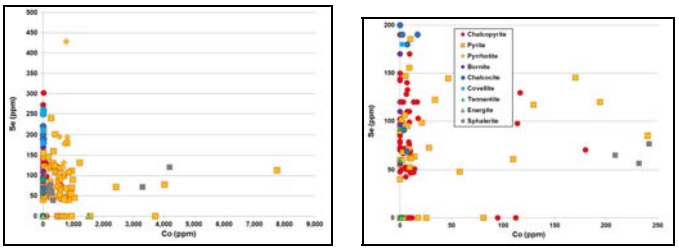

Figure 2. Plot of selenium versus cobalt in sulfide minerals analyzed in this study (representing 243 spot analyses of nine sulfide minerals in 11 ore deposits). Values below the detection limits are plotted as zero in this and following graphs. The left plot includes all data, whereas the right plot illustrates the distribution at low concentrations.

Indium & Silver

Silver and indium are particularly concentrated in many chalcopyrites and in enargite (Fig. 4). Some deposits tend to be more enriched than others in these trace elements. For example, chalcopyrite from Pumpkin Hollow ishighly enriched in silver (spot analyses ranging from 44 to 119 ppm) with variable indium contents (7.9 to 63 ppm), whereas the chalcopyrite from the Grasberg porphyry sample is relatively low in both elements (Fig. 5).

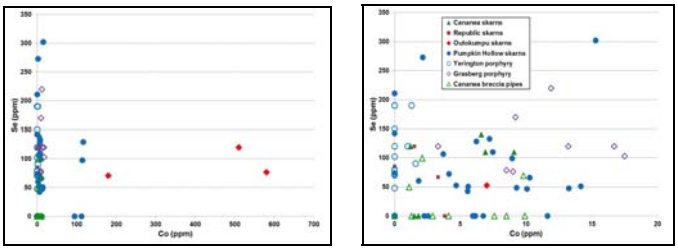

Figure 3. Plot of selenium versus cobalt in chalcopyrite samples (representing 84 spot analyses from eight ore deposits, including two Cananea breccia pipes). Values below the detection limits (1.6 ppm Co and 39 ppm Se in the Pumpkin Hollow samples, 1 ppm Co and 44 ppm Se in other samples) are plotted as zero.

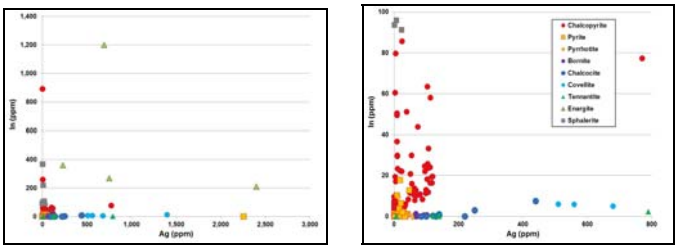

Figure 4. Plot of indium versus silver in sulfide minerals analyzed in this study.

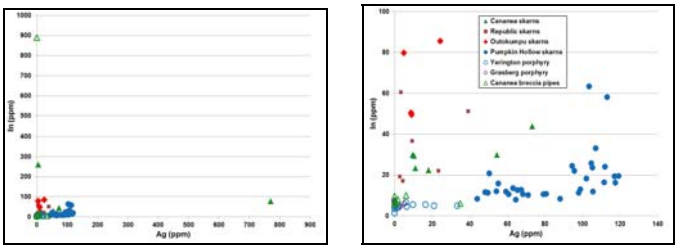

Figure 5. Plot of indium versus silver in chalcopyrite samples. Values below the detection limits (1.1 ppm Ag) are plotted as zero; no samples were below the detection limit for indium (0.3 ppm).

Tellurium

SEM analyses combined with heterogeneous concentrations measured in grains by LA-ICP-MS suggest that the dominant mode of occurrence of tellurium is micron-scale mineral grain inclusions (Table 3, Fig. 6). Grains are typically hosted within chalcopyrite or other copper phases, with lesser enrichment in pyrite, pyrrhotite, and sphalerite. The inclusions generally contain variable amounts of bismuth (Fig. 6), but also locally contain silver or lead (Fig. 7, 8).

One exception may be tellurium in tennantite from Chuquicamata, where all five spot analyses have high tellurium (from 19 to 220 ppm). Bismuth is also high in these five analyses (3.8 to 150 ppm). Bismuth, thallium, mercury, and silver are particularly high in the enargite from the Capote breccia pipe at Cananea (up to 5000 ppm Bi, 190 ppm Tl, 1300 ppm Hg, and 2400 ppm Ag), and tellurium and gold are also enriched in this mineral (up to 11 ppm Te and 2.8 ppm Au).

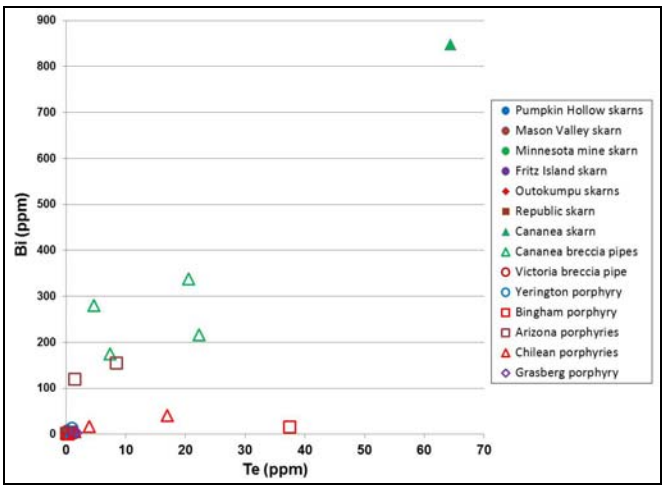

Figure 6. Plot of bismuth versus tellurium in whole-rock ore samples from porphyry copper systems.

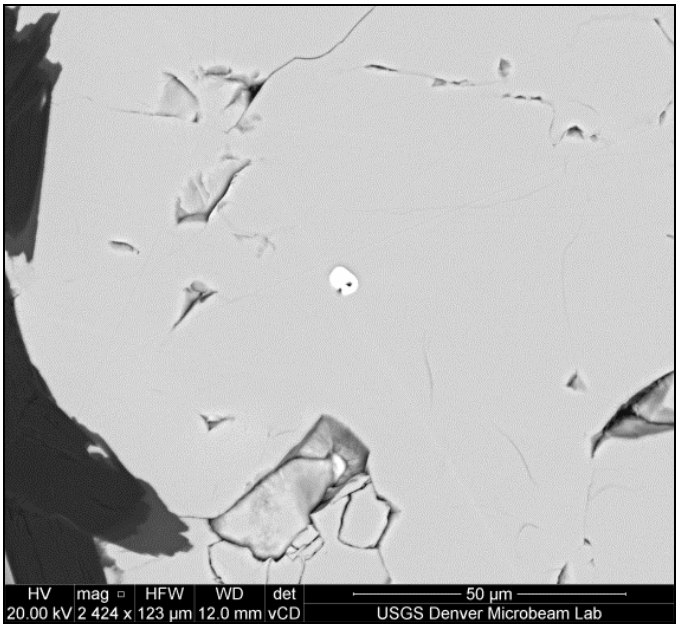

Figure 7. SEM image from Pumpkin Hollow sample NC08-39-1183 of tellurium-silver-bismuth mineral inclusion (bright spot in center) within chalcopyrite

Gold

Gold was detected only erratically in these samples, suggesting it occurs as small inclusions of native gold rather than in solid solution in other mineral phases (Fig. 9).An exception may be covellite from the Colorada breccia pipe at Cananea. The highest gold value measured in the sulfide minerals analyzed in this study is 41 ppm;that samplealso contains 1,400 ppm silver. Although the gold and silver may occur as submicroscopic electrum grains in this sample, it is noteworthy that all four spot analyses of this mineral are consistently high in both elements (Table 6).

Bismuth and Lead

Bismuth and lead are locally concentrated in some chalcopyrites, particularly in samples from the Yerington and Grasberg porphyry copper deposits (Fig. 10), although these occurrences may be as submicroscopic grains of bismuth-lead minerals with or without silver or tellurium. A single chalcopyrite analysis from the Elisa skarn deposit at Cananea has high lead as well as high gallium, selenium, silver, antimony, and mercury relative to other chalcopyrite analyses from the same deposit. This suite of elements may indicate that the analysis included submicroscopic inclusions of other minerals.

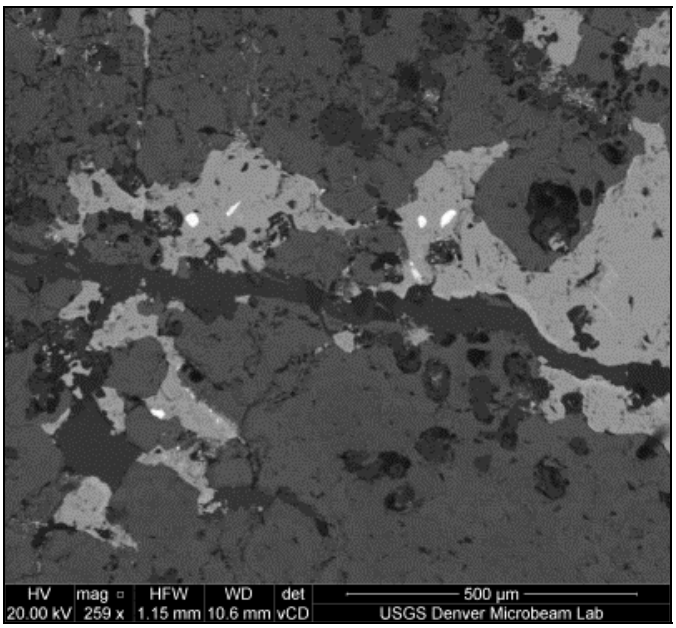

Figure 8. SEM image of light gray chalcopyrite with slightly lighter gray bornite rims along the fracture, Sample 0D-20023 from the Elisa mine, Cananea, Sonora, Mexico. The bright spots are Ag-Te inclusions within the chalcopyrite.

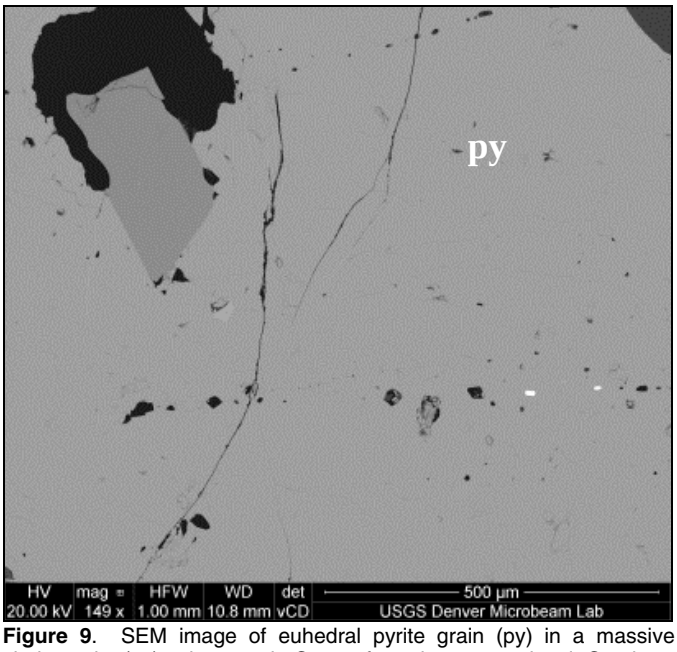

Figure 9. SEM image of euhedral pyrite grain (py) in a massive chalcopyrite (cp) vein, sample Gras-1 from the 3975-m level, Grasberg mine, Iran Jaya, Indonesia. Note the two fine white inclusions of gold below the cp label.

Cadmium

Cadmium substitutes for zinc, especially in sphalerite (Fig. 11), the primary ore mineral for zinc, which is why most global cadmium production is a byproduct of zinc production. Given their similarities in atomic radii (1.28Å for Cu, 1.38Å for Zn, 1.54Å for Cd), cadmium and zinc may also substitute for copper in chalcopyrite, as implied by locally high concentrations of these elements (Fig. 12). Although the spot mineral analyses by LA-ICP-MS specifically avoided inclusions of sphalerite within chalcopyrite grains, it is possible that submicroscopic inclusions of sphalerite have been included in the volume of analyzed material. Interestingly, chalcopyrite samples with relatively high cadmium tend to also have high zinc, but many of the high-zinc samples do not contain cadmium above the detection limit (Fig. 12).

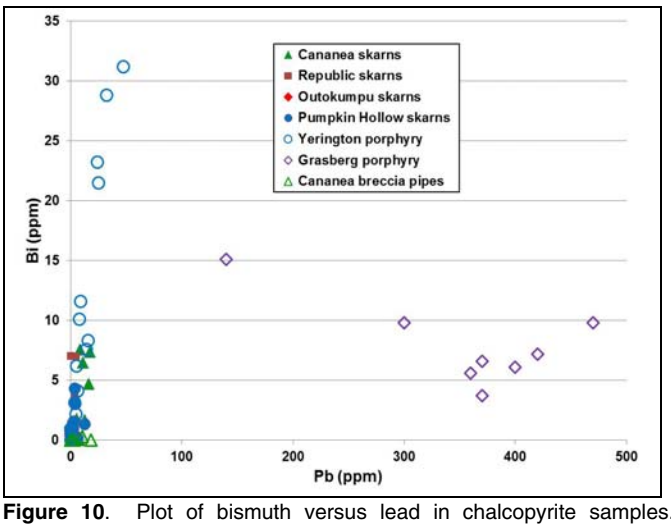

Figure 10. Plot of bismuth versus lead in chalcopyrite samples. Values below the detection limits (0.4 ppm Pb and 0.2 ppm Bi in the Pumpkin Hollow samples, 3 ppm Pb and 0.27 ppm Bi in other samples) are plotted as zero.

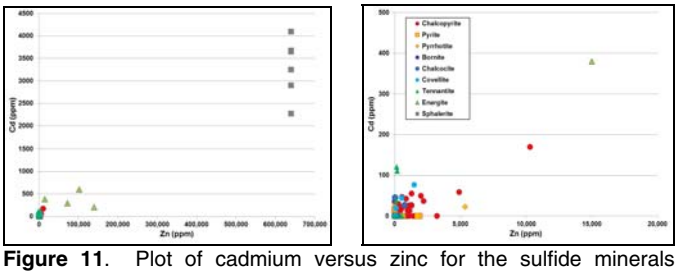

Figure 11. Plot of cadmium versus zinc for the sulfide minerals analyzed in this study. Note that the zinc value was set at 64%, the stoichiometric value for sphalerite, which was used as an internal standard during the analysis. Values below the detection limits are plotted as zero.

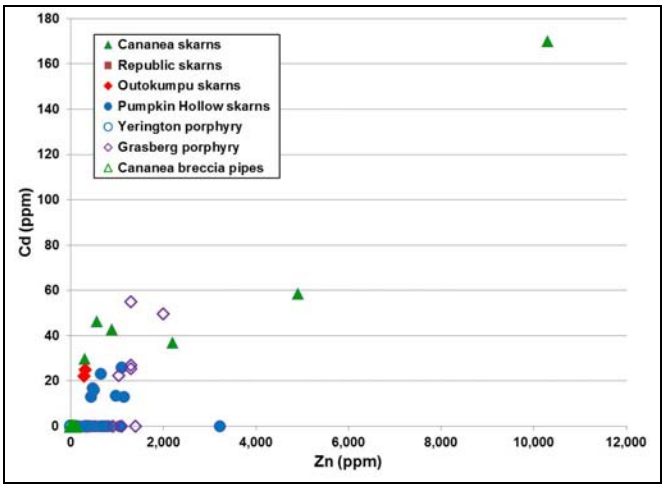

Figure 12. Plot of cadmium versus zinc in chalcopyrite samples. Values below the detection limits (13 ppm Cd in the Pumpkin Hollow samples, 11 ppm Zn and 20 ppm Cd in other samples) are plotted as zero.

Cobalt and Nickel

Cobalt and nickel are locally enriched in pyrite, pyrrhotite, and sphalerite (Fig. 13). Cobalt in particular is concentrated in the Pumpkin Hollow and Grasberg samples, with nickel concentrated in the Pumpkin Hollow samples and not the Grasberg sample (Fig. 14). All four orebodies (Fig. 15) sampled at Pumpkin Hollow contain pyrites that are high in cobalt and nickel as well as low in both elements.

Four separate paragenetic pyrite phases have been identified in the Pumpkin Hollow samples. The first is a clean, euhedral pyrite. This phase typically has a slightly higher reflectance and is almost exclusively in contact with chalcopyrite (Fig. 16A). The second phase is a broken, irregular, anhedral pyrite that is locally replaced by pyrrhotite along fractures and grain boundaries (Fig. 16B). The third phase is a ratty, almost sanded textured pyrite with parallel streaks/laminations (Fig. 16C). The fourth phase is a late-stage euhedral vein pyrite (Fig. 16D).

Each pyrite phase is distinguishable based on its cobalt and nickel contents. The first euhedral phase invariably contains the highest cobalt values (up to 7800 ppm), with low nickel values (50 ppm Ni in the highest Co sample). There does not appear to be a uniformly distributed concentration of cobalt between grains, nor is there any observed cobalt zoning within grains. The ratio of cobalt to nickel ranges from 3:1 up to 25:1. Due to the high cobalt content, this phase is identifiable megascopically as being whiter than the other pyrite phases. The same is true microscopically; this phase appears brighter than the other pyrite phases. The broken, irregular pyrite (phase two) typically contains the highest nickel values (up to 9100 ppm), with lesser cobalt (850 ppm Co in the highest Ni sample). This phase is the most common in all of the samples. The cobalt to nickel ratios average about 1:10, and the ratio is more consistent than observed in the previous pyrite phase. This phase of pyrite also has the highest average concentrations of selenium, but the concentrations are highly variable. The third phase is limited in terms of occurrence and may be the result of alteration rather than a distinct phase. The geochemistry most closely resembles the broken pyrite phase, but minor amounts of silver are also present. There does not appear to be any zoning of elements within the grains. The fourth phase of pyrite is a late-stage vein pyrite associated with quartz-calcite veins. This phase occurs as euhedral crystals with local growth zoning. It is essentially barren, with only trace amounts of cobalt and silver locally. No trace elements of economic interest occur within this phase.

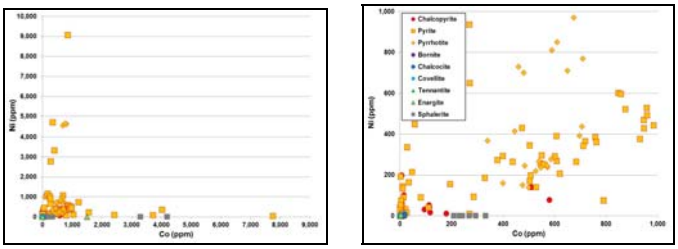

Figure 13.Plot of nickel versus cobalt for the sulfide mineral analyzed in this study.

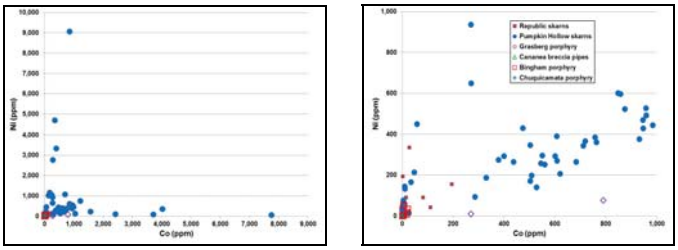

Figure 14. Plot of nickel versus cobalt in pyrite samples (representing 99 spot analyses from six ore deposits). Values below the detection limits (1.6 ppm Co and 5.9 ppm Ni in the Pumpkin Hollow samples, 1.0 ppm Co and 3 ppm Ni in other samples) are plotted as zero.

Cobalt and nickel are generally higher in copper-iron skarn deposits than in porphyry copper deposits, but in order to support this finding additional samples would need to be analyzed (Fig. 17). Specifically, the Yerington porphyry copper deposit contains less nickel and cobalt relative to the Yerington district skarn deposits at Pumpkin Hollow and Mason Valley.

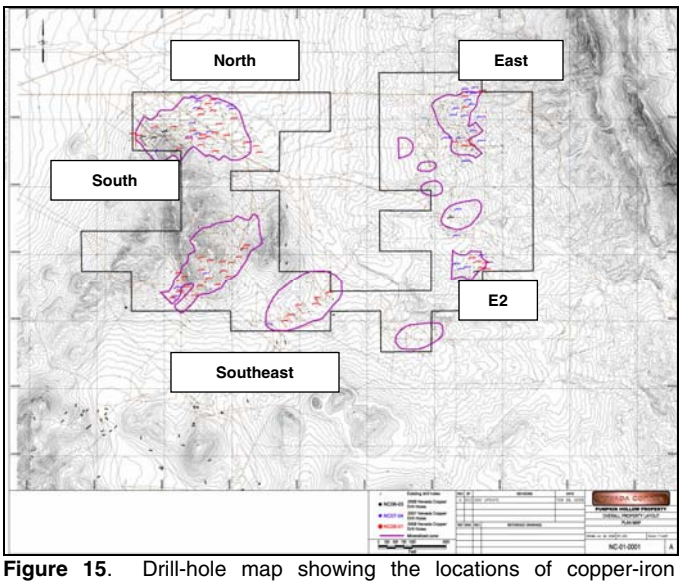

Figure 15. Drill-hole map showing the locations of copper-iron deposits at Pumpkin Hollow, Lyon County, Nevada (courtesy of Nevada Copper Corporation). The purple outlines represent mineralized zones. Samples were analyzed from the North (diamond drill hole, DDH NC08-20), South (DDH NC08-19 and DDH NC08-25), East (DDH NC08-49), and E2 (DDH NC08-39) deposits.

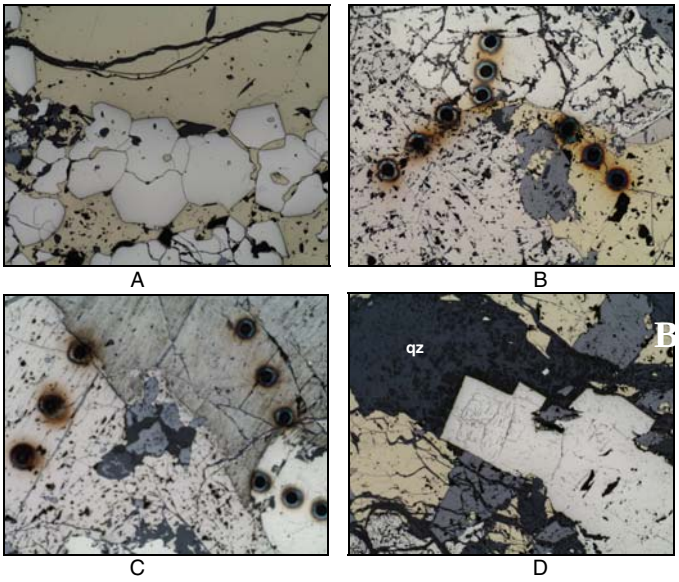

Figure 16. Photomicrographs A) Sample NC08-49-1665 series of interlocking euhedral pyrite grains (light gray) overgrown and locally replaced by chalcopyrite (yellow), 0.85 mm field of view (FOV); B) Sample NC08-20-1213 broken pyrite (upper, white mineral) adjacent to pyrrhotite (brown) and chalcopyrite (yellow), 1.70 mm FOV; C) Sample NC08-39-1183 ratty, sanded pyrite (left, light gray) only rarely observed, 1.70 mm FOV; D) Sample NC08-20-1213 late-stage barren euhedral vein pyrite (white) with quartz (qz) cutting chalcopyrite (yellow)-magnetite (dark gray) rods, 1.70 mm FOV. Circular spots are laser ablation pits.

Gallium

Gallium is locally concentrated in some magnetite deposits (Fig 18). Because of the similarity in ionic radii of Ga^{3+} (0.62 Å) and Fe^{3+} (0.64 Å), the gallium is likely in solid solution in the magnetite and might be recoverable during reduction of iron in magnetite to make steel. Other trace elements that are likely in solid solution in magnetite include titanium, vanadium, aluminum, and silicon (Figs. 19 and 20). Magnetite samples with relatively low gallium contents tend to be also low in magnesium, aluminum, titanium, and silicon (Table 4). Among the spot analyses from the Pumpkin Hollow orebodies, the analysis with the lowest gallium concentration is from the rim of a magnetite grain, suggesting that the late-stage hydrothermal fluid was probably lower in temperature than the earlier fluid from which the bulk of the magnetite grains were precipitated.

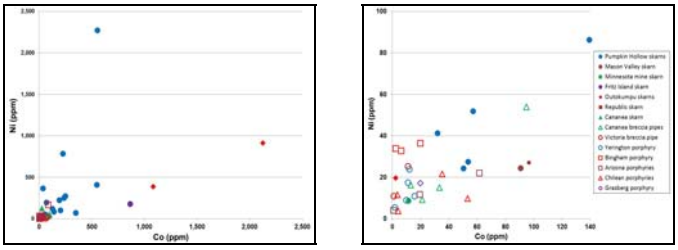

Figure 17. Plot of nickel versus cobalt in whole-rock ore samples from porphyry copper systems.

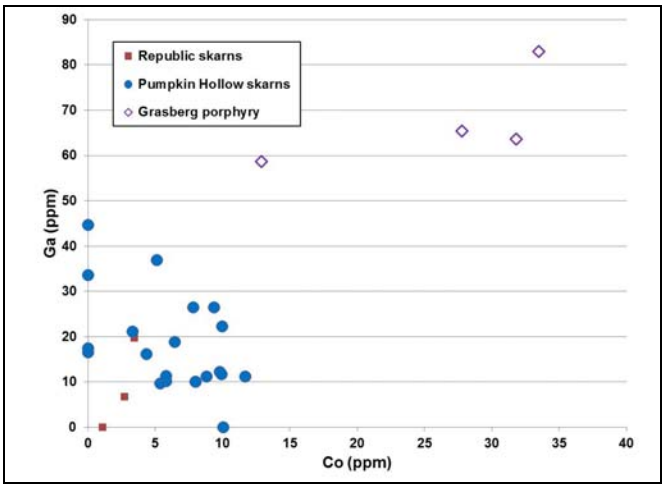

Figure 18. Plot of gallium versus cobalt in magnetite (representing 29 spot analyses from three ore deposits). Values below the detection limits (3 ppm Co and 5 ppm Ga in the Pumpkin Hollow samples, 2.0 ppm Co and 6 ppm Ni in other samples) are plotted as zero.

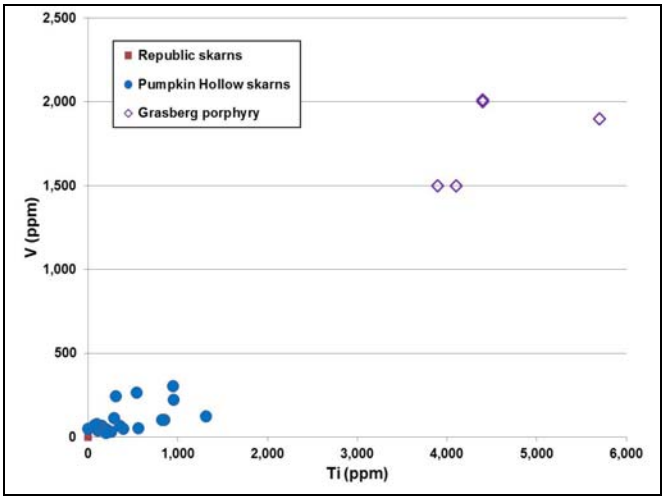

Figure 19. Plot of vanadium versus titanium in magnetite. Values below the detection limits (58 ppm Ti in the Pumpkin Hollow samples, 77 ppm Ti and 11 ppm V in other samples) are plotted as zero.

CONCLUSIONS AND RECOMMENDATIONS

This reconnaissance study demonstrates that minerals from porphyry copper systems host a wide range of critical and strategic trace elements. At current prices, many of these elements are sufficiently enriched to warrant investigation into metallurgical recovery as byproducts of the major elements. For example, the Pumpkin

Hollow orebodies (Table 8) will likely receive credits for silver and indium, and possibly selenium, in concentrates of chalcopyrite. If metallurgically feasible, gallium might also be recovered from magnetite concentrates. Moreover, pyrite and/or pyrrhotite concentrates from Pumpkin Hollow could be valuable sources of cobalt, nickel, and selenium. Clearly more work needs to be done to determine whether certain elements are more concentrated in certain types of copper ore-forming systems and types of deposits. Also, more work needs to be done on the distribution of trace elements in individual minerals.

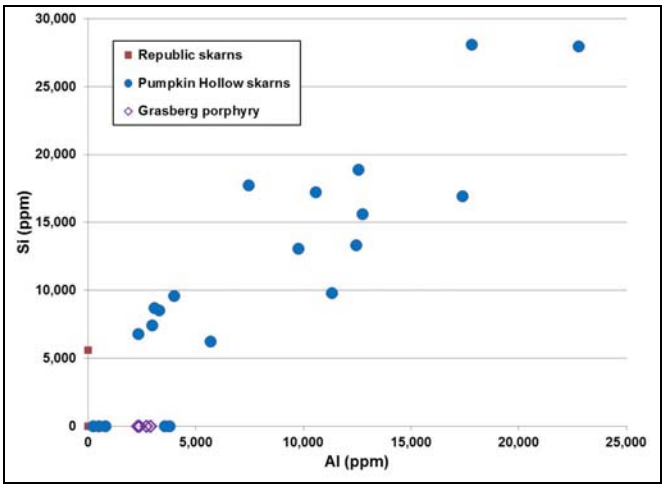

Figure 20. Plot of silicon versus aluminum in magnetite. Values below the detection limits (5360 ppm Si and 254 ppm Al in the Pumpkin Hollow samples, 4710 ppm Si and 388 ppm Al in other samples) are plotted as zero.

Table 8. Statistics on selected trace elements in magnetite, pyrite, pyrrhotite, and chalcopyrite in ores at the Pumpkin Hollow iron-copper deposits, Nevada (ppm, or grams per tonne, by weight); st. dev. = standard deviation.

Phase (number of analyses)	Element	Ave. ± st. dev.	Range	Value ($/tonne)[3]
Magnetite (22)	Ga	17 ± 11	<4.7 to 45	12
Pyrite (69)[1]	Co	650 ± 1120	<2 to 7800	26
	Ni	560 ± 1270	<6 to 9100	13
	Se	74 ± 48	<39 to 190	11
Pyrrhotite (20)	Co	570 ± 120	340 to 810	23
	Ni	1300 ± 1700	140 to 4600	30
	Se	100 ± 97	<39 to 430	14
	Te	4 ± 6	<7 to 16	1.40
Chalcopyrite (33)[2]	Zn	670 ± 520	150 to 3200	1.60
	Ag	84 ± 24	44 to 120	93
	In	18 ± 12	7.9 to 63	13
	Se	71 ± 76	<39 to 300	10
	Te	3 ± 5	<7 to 23	1.10

[1] excluding one sample with high Ag content (2260 ppm), which may indicate another phase.
[2] including only samples with >29% Cu, to avoid mixtures with other phases.
[3] estimated value of contained metal in concentrate of these minerals, using average prices in 2011 from the U.S. Geological Survey (2012): Co ($40/kg), Zn ($2.34/kg), Ga ($700/kg), In ($720/kg), Ni ($23/kg), Se ($143/kg), Ag ($1,109/kg), Te ($360/kg).

ACKNOWLEDGMENTS

We thank Greg French and Hank Ohlin of Nevada Copper Corporation for access to samples, maps, cross sections, and geochemical data from the Pumpkin Hollow orebodies. We also thank Dean Jeffrey Thompson of the College of Science at the University of Nevada, the Nevada Bureau of Mines and Geology, and the U.S. Geological Survey for providing financial support for this work. Stanford University donated its ore deposits collection to the Mackay School of Earth Sciences and Engineering at the University of Nevada, where it is available, along with recent additions, for research.

REFERENCES

1. Anderson, C.A. 1950. Alteration and metallization in the Bagdad porphyry copper deposit, Arizona.*Economic Geology* 45:609-628.
2. Baker, A. 1960. Chalcopyrite blebs in sphalerite at Johnson Camp, Arizona.*Economic Geology* 55:387-398.
3. Bushnell, S.E. 1988. Mineralization at Cananea, Sonora, Mexico, and the paragenesis and zoning of breccia pipes in quartz feldspathic rock.*Economic Geology* 83:1760-1781.
4. Carten, R.B. 1986. Sodium-calcium metasomatism: chemical, temporal, and spatial relationships at the Yerington, Nevada, porphyry copper deposit.*Economic Geology* 81:1495-1519.
5. Dilles, J.H. 1987. Petrology of the Yerington batholith, Nevada: evidence for evolution of porphyry copper ore fluids.*Economic Geology* 82:1750-1789.
6. Doebrich, J.L., Garside, L.J., and Shawe, D.R., 1996. *Characterization of mineral deposits in rocks of the Triassic to Jurassic magmatic arc of western Nevada and eastern California*:U.S. Geological Survey Open-File Report 96-9, 107 p.
7. Eggert, R.G., Carpenter, A.S., Freiman, S.W., Graedel, T.E., Meyer, D.A., McNulty, T.P., Moudgil, B.M., Poulton, M.M., and Surges, L.J. 2008.*Minerals, critical minerals, and the U.S. economy*: National Research Council of the National Acadamies, National Academies Press, Washington, D.C., 245 p.
8. Einaudi, M.T. 1977. Petrogenesis of the copper-bearing skarn at the Mason Valley mine, Yerington district, Nevada.*Economic Geology* 72:769-795.
9. Emsbo, P., Koenig, A.E., Bryant, D, Lowers, H, and Van Gosen, B. 2010. Quick assessment of rare metals in ore deposits: prototype for a national assessment. *Technical Program of the Society for Mining, Metallurgy and Exploration* 2010 annual meeting, Phoenix, Arizona, p. 88.
10. Harris, N. B. and Einaudi, M. T. 1982. Skarn deposits in the Yerington district, Nevada: metasomatic skarn evolution near Ludwig.*Economic Geology* 77:877-898.
11. Jaffe, R., Price, J.G., Ceder, G., Eggert, R., Graedel, T., Gschneidner, K., Jr., Hitzman, M., Houle, F., Hurd, A., Kelley, R., King, A., Milliron, D., Skinner, B., and Slakey, F. 2011.*Energy critical elements: securing materials for emerging technologies*: Report by the American Physical Society Panel on Public Affairs and the Materials Research Society, 23 p.
12. Klemm, L.M, Pettke, T., and Heinrich, C.A., and Campo, E. 2007. Hydrothermal evolution of the El Teniente deposit, Chile: porphyry Cu-Mo ore deposition from low-salinity magmatic fluids.*Economic Geology* 102:1021-1045.
13. LaPointe, D.D., Tingley, J.V., and Jones, R.B. 1992.*Mineral resources of Elko County, Nevada*: Nevada Bureau of Mines and Geology Bulletin 106, 236 p.
14. Latiff, R.H., Reininga, H.M., Adkins, C., Blue, B.E., Flamm, K.S., Frase, K.G., Gessaman, D.E., Gonczy, S.T., Keeney, R.L., Kielty, E.R., Looney, J.P., Mitchell, G.R., Mory, P.C., Mowery, D.C., Mueller, D.B., Singh, M.M., Walsh, K.A., and Williams, J.C. 2008.*Managing materials for a twenty-first century military*: National Research Council of the National Acadamies, National Academies Press, Washington, D.C., 189 p.
15. Livingston, D.E., Mauger, R.L., and Damon, P.E. 1968. Geochronology of the emplacement, enrichment, and preservation of Arizona porphyry copper deposits.*Economic Geology* 63:30-36.
16. Longerich, H., Jackson, S., and Gunther, D. 1996. Laser ablation inductively coupled plasma mass spectrometric transient signal data acquisition and analyte concentration calculation.*Journal of Analytical Atomic Spectrometry*11: 899-904.

17. Loukola-Ruskeeniemi, K. 1999. Origin of black shales and the serpentinite-associated Cu-Zn-Co ores at Outokumpu, Finland.*Economic Geology* 94:1007-1028.

18. Lowell, J.D. and Guilbert, J.M. 1970. Lateral and vertical alteration-mineralization zoning in porphyry ore deposits.*Economic Geology* 65:373-408.

19. Meinert, L.D. 1982. Skarn, manto, and breccia pipe formation in sedimentary rocks of the Cananea mining district, Sonora, Mexico.*Economic Geology* 77:919-949.

20. Moore, J.G. 1969.*Geology and mineral deposits of Lyon, Douglas, and Ormsby Counties, Nevada*: Nevada Bureau of Mines and Geology Bulletin 75, 53 p.

21. Ossandon, G.C., Freraut, R.C., Gustafson, L.B., Lindsay, D.D., & Zentilli, M. 2001. Geology of the Chucuicamata mine: a progress report.*Economic Geology* 96:249-270.

22. Peltola, E. 1978. Origin of Precambrian copper sulfides of the Outokumpu district, Finland.*Economic Geology* 73:461-477.

23. Pollard, P.J., Taylor, R.G., & Peters, L. 2005. Ages of intrusion, alteration, and mineralization at the Grasberg Cu-Au deposit, Papua, Indonesia.*Economic Geology* 100:1005-1020.

24. Proffett, J.M., Jr., and Dilles, J.H. 1984. Geologic map of the Yerington district, Nevada: *Nevada Bureau of Mines and Geology Map* 77, 1:24,000-scale.

25. Seedorff, E., Barton, M.D., Stavast, W.J.A., & Maher, D.J. 2008. Root zones of porphyry systems: extending the porphyry model to depth.*Economic Geology* 103:939-956.

26. Sindeeva, N. D. 1964.*Mineralogy and types of deposits of selenium and tellurium*: John Wiley & Sons, Inc., New York, 363 p.

27. Spencer, A.C. 1908.*Magnetite deposits of the Cornwall types in Pennsylvania*: U.S. Geological Survey Bulletin 359, 102 p.

28. U.S. Geological Survey 2012.*Mineral commodity summaries 2012*: U.S. Geological Survey, Reston, Virginia, 198 p.

29. Wilson, S.A., Ridley, W.I., and Koenig, A.E. 2002. Development of sulfide calibration standards for the laser ablation inductively coupled plasma mass spectrometry technique.*Journal of Analytical Atomic Spectrometry* 17:406-409.

30. Yano, R.I. 2012. Trace element distribution in chalcopyrite-bearing porphyry and skarn deposits. M.S. thesis, University of Nevada, Reno, 92 pg.

APPENDIX

Table 2. Bulk-rock analyses of ores by LA-ICP-MS (values in ppm by weight).

Sample number	S	V	Cr	Mn	Fe	Co	Ni	Cu	Zn	Ga	Ge	As	Se	Mo	Ag	Cd	In	Sb	Te	Au	Hg	Tl	Pb	Bi
PHNC08-39-1183	199226	4.2	6.4	135	227694	139	86	135000	965	1.3	0.28	0.92	32	0.29	46	12	5.5	0.52	2.0	0.013	13	0.015	28	1.7
PHNC08-39-1216	140152	12	50	495	277388	249	272	15000	57	3.5	0.58	4.8	26	1.2	4.5	1.4	5.0	1.0	1.3	0.007	8.1	0.002	16	4.3
PHNC08-39-1224	299455	3.0	26	247	288413	202	103	177000	1374	0.67	0.40	6.1	50	1.2	52	9.0	6.5	0.75	2.0	0.047	14	0.11	29	2.2
PHNC08-39-1269	106454	14	20	260	244388	127	119	26000	105	2.8	0.52	7.2	53	6.7	11	1.5	1.1	1.9	0.54	0.021	5.0	0.015	3.3	1.5
PHNC08-20-1213	423648	33	52	213	558020	226	785	150000	586	6.1	0.65	476	71	2.9	51	21	22	5.6	2.4	0.12	37	0.037	38	1.8
PHNC08-20-1206	274083	24	22	154	339964	235	254	180000	834	4.2	0.64	47	43	1.4	55	14	13	1.2	2.7	0.051	20	0.020	10	1.6
PHNC08-20-1194	180572	30	14	144	241054	192	222	90000	435	4.1	0.42	35	33	0.95	32	5.3	8.5	1.5	4.0	0.024	15	0.030	9.7	3.6
PHNC08-20-1193	51726	41	71	150	192677	57	52	30000	145	5.6	0.48	52	9.7	2.1	10	1.5	2.4	1.1	0.29	0.017	4.2	0.015	6.8	0.50
PHNC08-19-1535	50563	44	42	142	251817	50	24	10000	35	11	0.40	6.8	3.4	2.3	3.8	0.45	0.54	1.12	0.23	0.031	4.1	0.18	5.1	0.49
PHNC08-19-1531	47139	30	42	121	204488	54	27	15000	57	7.2	0.28	5.2	3.7	1.4	5.6	0.67	1.5	0.46	0.16	0.017	4.0	0.084	3.8	0.50
PHNC08-25-627	210399	71	57	140	208346	349	69	70000	144	1.9	0.83	111	27	0.89	31	2.6	3.2	4.0	2.2	0.41	16	0.070	8.2	8.2
PHNC08-25-640	54927	107	94	347	120278	32	41	20000	54	8.1	0.38	2.4	6.4	1.4	9.0	0.55	0.23	0.62	0.19	0.015	3.1	0.014	3.3	0.52
PHNC08-49-1661	180919	16	73	298	167349	37	368	155000	125	2.8	0.83	5.6	43	2.3	39	2.2	4.6	1.7	3.2	0.042	11	0.010	6.0	1.4
PHNC08-49-1665	578931	3.1	22	109	527002	553	2273	65000	56	0.79	0.45	226	148	1.3	27	1.1	7.5	2.3	18	0.073	12	0.0096	7.4	8.2
PHNC08-49-1687	66203	92	35	272	164884	69	195	30000	128	4.9	0.51	62	9.4	1.1	9.0	2.8	0.96	2.9	0.51	0.51	5.2	0.010	4.7	1.2
PHNC08-49-1703	244626	41	75	131	322160	547	410	70000	353	5.0	0.34	44	39	2.4	23	8.1	2.9	1.5	2.1	0.084	12	0.026	5.0	9.3
MVHD	16567	2.4	21	830	45431	91	24	3980	136	0.61	0.46	6.3	6.6	2.0	0.46	0.28	0.06	0.25	0.09	0.014	0.49	0.039	13	4.7
STSG	7435	9.8	3.6	250	53533	12	8.7	1500	185	5.3	0.90	5.8	2.7	140	1.6	0.23	0.10	0.44	0.18	0.011	2.3	0.033	4.8	2.9
OD13152	100946	13	93	469	232602	864	178	55032	1022	4.1	0.77	207	13	1.6	1.8	2.1	4.6	0.42	0.85	0.068	33	0.53	63	1.8
OD31730	52120	38	40	284	55853	2.4	20	14800	2668	16	1.3	49	9.7	9.2	14	6.8	0.49	7.0	0.60	0.040	13	0.53	559	0.41
OD31756	184609	10	40	325	158040	1083	389	75300	9129	2.0	1.3	12	35	5.7	12	19	11	3.4	0.40	0.45	53	0.11	32	2.8
OD31759	225462	45	101	1102	241473	2125	915	14100	1141	4.3	0.64	18	17	2.3	2.4	1.9	1.2	1.1	0.74	0.034	11	0.30	24	0.73
OD14895	199185	12	42	7167	84150	97	27	41100	219579	7.6	3.4	16	40	8.7	30	547	32	1.0	1.3	0.036	20	0.063	12	10
OD20023	92290	15	28	6482	121432	27	128	83000	1046	6.3	4.0	51	31	1.4	234	4.4	8.0	7.5	64	0.13	9.2	0.19	2384	848
OD20021	318202	5.4	18	1129	203039	21	9.2	318963	12917	4.2	23	22511	2.5	2.7	1344	29	122	73	4.7	0.56	267	8.1	2561	280
OD20104	268234	57	77	13	89430	13	16	411000	547	9.4	2.5	1406	126	113	400	1.6	2.4	41	21	11	13	2.1	32	338
OD20001	307515	333	22	34	64225	33	15	185000	281	16	4.0	124	57	3135	185	2.4	1.9	1.7	7.4	0.54	8.0	0.71	92	175
OD20003	281421	8.8	48	115	164578	95	54	448212	595	2.2	0.60	492	76	3.1	367	4.0	5.6	12	22	4.4	58	0.74	102	216
JP205-33	159240	18	67	186	120977	11	25	162093	369	1.4	0.51	129	32	3.0	72	2.8	7.8	17	1.2	0.044	21	1.3	10	4.4
JP205-30	218183	1.1	13	38	174746	1.0	11	220001	238	1.8	0.89	49	0.84	0.59	9.6	6.5	13	8.9	0.19	0.030	17	3.1	6.1	7.2
Yer-5	13635	35	128	104	19007	11	17	18000	357	13	1.2	22	13	2.9	9.9	1.8	0.52	1.9	1.0	0.036	1.0	0.34	20	12
Yer-6	88024	149	186	190	91359	12	24	68000	103	18	1.0	2.5	25	1.9	5.9	0.71	1.3	0.40	0.92	0.057	1.1	0.28	12	4.0
Yer-3	13956	76	94	123	26516	16	11	4120	76	25	1.2	12	2.7	3.4	1.3	0.09	0.30	0.93	1.0	0.016	0.88	0.96	12	3.7
Yer-4	11100	62	51	61	16618	10	8.9	3066	75	12	0.78	44	2.7	1.3	2.2	0.26	0.28	0.16	0.09	0.005	5.2	0.49	4.3	1.8
OD10808	31239	29	25	79	9053	1.8	5.5	531000	204	8.8	0.87	4.98	116	2.3	8.1	0.11	0.14	2.3	0.41	0.029	4.1	0.19	15	5.2
JP205-5A	2024	102	87	44	7068	2.4	34	500	56	14	1.2	1.84	0.62	133	0.73	0.09	0.08	0.26	0.16	0.005	0.32	0.83	18	1.9
JP205-2	22477	86	77	267	32170	20	36	290	85	10	1.3	2.76	2.1	1.8	0.49	0.07	0.11	0.16	0.40	0.009	0.50	0.97	27	1.1
JP205-5B	3827	99	78	74	12990	6.2	33	1490	41	12	1.2	25	1.5	263	0.95	0.03	0.03	0.19	0.12	0.040	0.42	0.83	8.1	1.6
OD9927	355450	40	112	16	317385	85	170	91397	212	7.5	2.1	277	108	47	29	0.54	0.21	6.1	37	0.31	1092	2.5	120	15
OD3673	595918	14	39	735	530098	0.86	4.1	60500	235	1.9	2.2	41	4.9	1	96	0.43	8.1	1.1	8.5	0.11	5.1	0.15	79	155
OD43579	110306	24	88	2749	100148	62	22	79700	2748	9.2	3.6	77	18	234	99	12	4.8	2.3	1.5	0.012	3.7	0.27	50	120
OD16922	12990	33	40	107	17648	19	12	1100	204	7.5	0.83	1.8	1.6	2.1	2.2	6.1	0.75	2.1	0.22	0.012	0.68	0.42	8.8	0.65
OD47214	137624	70	9.1	16.6	44987	4.2	3.8	42500	233	48	69	12580	2.6	29	157	3.5	11	470	17	0.13	31	0.45	1495	41
OD21422	279505	44	14	71	235321	53	9.8	12800	98	13	2.6	3.9	17	15	8.8	0.22	0.25	0.84	1.5	0.027	2.8	0.17	1883	4.8
OD28536	139513	141	93	119	90761	35	22	87100	147	10	1.4	56	10	87	10	0.76	0.52	1.0	0.36	0.018	3.7	0.51	2.6	0.43
OD28539	38211	66.9	65	165	15721	3.5	12	11800	279	7.5	1.2	100	1.8	5.5	4.1	0.63	0.72	4.0	3.9	0.025	0.95	0.45	67	17
Gras-1	51947	74	150	440	87894	20	17	22700	432	12	2.4	12	16	12	8.2	1.4	0.65	0.68	1.7	0.54	1.6	0.28	43	3.3

APPENDIX (cont'd)

Table 3. Spot analyses of chalcopyrite by LA-ICP-MS (values in ppm by weight). In this and other tables, values below the detection limit are listed as zero; na = not analyzed.

Locality	Sample #	Grain	S	Mn	Fe	Co	Ni	Cu	Zn	Ga	Ge	As	Se	Ag	Cd	In	Sb	Te	Au	Hg	Tl	Pb	Bi
Yerington	YER-6	1	330000	0	300000	1.6	0	310000	0	0	0	0	90	9.8	0	5.5	0	0	0.23	0	0	25	22
		1	330000	0	300000	0	0	320000	0	0	0	0	0	17	0	5.5	0	0	0.22	0	0	24	23
		1	330000	0	300000	0	0	310000	0	0	0	0	0	6.4	0	4.5	0	0	0.25	250	0	8.8	12
		2	320000	0	300000	0	0	310000	0	0	0	0	78	0	0	6.9	0	0	0	0	0	0	1.0
		2	330000	0	300000	0	0	310000	0	0	0	0	102	0	0	4.7	0	0	0	0	0	0	0
		2	350000	6.2	300000	0	0	310000	0	0	0	0	120	2	0	5.1	0	0	0	0	0	5.1	6.2
		3	320000	7.3	300000	0	0	305000	0	0	0	0	190	1.5	0	3.9	0	0	0	0	0	14	7.6
		3	330000	0	300000	0	0	305000	15	0	0	0	80	0	0	4.6	0	0	0	0	0	4.9	2.2
		3	330000	0	300000	0	0	310000	14	0	0	0	190	2.1	0	4.3	0	0	0	0	0	3.4	3.1
		4	340000	0	300000	0	0	310000	0	0	0	0	71	21	0	5	0	0	0.21	0	0	32	29
		4	320000	5.5	300000	0	0	320000	0	0	0	0	48	33	0	5	0	20	0	220	0	48	31
		4	310000	0	300000	1	0	320000	0	0	5.8	0	120	5.9	0	6.7	0	0	0	0	0	7.6	10
		4	340000	0	300000	0	3.4	320000	0	0	0	0	150	0	0	4.6	0	0	0	170	0	0	0.8
		5	330000	0	300000	1.3	0	320000	0	0	0	0	190	0	0	3.4	0	0	0	0	0.31	16	8.3
		5	360000	0	300000	0	0	300000	0	0	0	0	72	0	0	1.4	0	0	0	0	0	6	4.1
Grasberg	Gras-1	1	360000	85	300000	13	6.7	320000	1040	3.7	0	0	120	5.3	22	5.9	0	0	1.6	0	0	470	9.8
		1	350000	28	300000	8.5	0	330000	1400	0	0	0	78.9	0	0	7.0	0	8.8	0	0	0	360	5.6
		1	340000	36	300000	12	0	310000	1300	0	14	0	220	0	26	6.7	0	12	0	0	0	420	7.2
		1	350000	18	300000	3.3	0	320000	910	4.8	4.9	0	120	2.9	0	4.6	0	0	0.41	0	0	140	15
		1	390000	21	300000	9	0	310000	1100	0	4.8	0	76.1	0	0	7.4	0	0	0	0	0.33	300	9.8
		2	340000	34	300000	18	0	310000	2000	0	4.7	0	103	0	50	7.6	0	0	0	0	0	370	6.6
		2	340000	33	300000	17	0	300000	1300	0	0	0	120	0	55	6.5	0	0	0	0	0	370	3.7
		3	360000	17	300000	9.2	0	300000	1300	3.4	0	0	170	0	27	5.1	0	0	0.23	0	0	400	6.1
Cananea Colorado	OD-20003	1	370000	16	300000	1.3	0	330000	0	0	0	0	0	6.1	0	10	0	0	0	0	0	0	0
		1	380000	15	300000	9.8	0	320000	110	0	0	0	70	35	0	6.1	0	0	0	0	0	18	0
		1	370000	0	300000	7.6	0	320000	23	0	0	0	0	0	0	6.7	0	0	0	0	0	0	0
		2	350000	28	300000	2.1	0	320000	75	0	0	0	100	0	0	9.6	0	0	0	0	0	10	0.32
		2	340000	0	300000	2.9	0	330000	22	0	0	0	0	0	0	5.9	0	0	0	176	0	0	0
		3	370000	0	300000	1.1	0	33000	39	0	0	0	50	1.7	0	8.0	0	9.3	0	0	0	0	0
		3	380000	0	300000	4.1	6.2	320000	47	3.1	0	0	0	0	0	5.9	0	0	0	0	0	0	0
		3	390000	0	300000	9.9	4.5	320000	0	0	0	0	0	0	0	6.0	0	0	0	240	0	0	0
		3	380000	0	300000	8.5	0	33000	37	4.6	0	0	0	1.2	0	6.1	0	0	0.20	0	0	0	0
Cananea Capote	OD-20021	3	350000	0	300000	0	0	320000	0	18	0	12	0	0	0	890	0	0	0	263	0	3.2	0
Cananea Elisa	OD-20023	4	390000	0	300000	0	4.2	320000	26	20	5.9	12	0	4.7	0	260	0	0	0	750	0	7.8	0
		1	390000	0	300000	1.8	0	320000	560	0	0	11	0	10	46	29	0	23	0	0	0	11	6.5
		1	370000	0	300000	6.9	0	330000	2200	0	0	15	110	9.6	37	30	0	0	0	500	0	5.2	1.8
		2	350000	0	300000	1.8	0	330000	880	0	0	0	0	11	43	23	2.3	0	0	430	0	8.2	7.6
		2	350000	0	300000	1.5	0	310000	300	0	0	0	0	18	30	22	0	0	0	270	0	16	4.7
		2	370000	0	300000	1.2	0	340000	300	0	0	0	120	54	0	30	1.3	0	0	340	0	13	1.7
		3	400000	31	270000	6.6	7.8	300000	4900	170	0	13	140	770	59	77	2.8	0	0.37	2400	0	3400	18
		3	370000	120	280000	9.1	4.8	300000	10300	0	0	0	110	73	170	44	0	0	0	1300	0	17	7.4
Republic	OD-14895	1	339000	0	300000	1.5	0	309000	53	0	0	8.6	120	23	0	22	0	0	0	0	0	0	7.0
		1	338000	0	300000	3.3	0	305000	280	0	0	0	67	2.8	0	19	1.39	8.6	0	0	0.36	0	0.9
			353000	0	300000	3.8	0	311000	115	0	0	0	0	4.4	0	17	0	0	0	0	0	3.6	3.7
		2	375000	0	300000	0	4.3	314000	32	0	0	0	0	3.4	0	61	0	0	0	0	0	3.3	4.3
		3	364000	0	300000	0	0	329000	71	0	0	0	85	9.3	0	37	0	0	0	0	0	0	1.3
		3	376000	0	300000	0	0	334000	141	0	7.1	0	144	39	0	51	1.7	0	0	0	0	4.8	7.0

APPENDIX (cont'd)

Table 3. Spot analyses of chalcopyrite by LA-ICP-MS, **continued**.

Locality	Sample #	Grain	S	Mn	Fe	Co	Ni	Cu	Zn	Ga	Ge	As	Se	Ag	Cd	In	Sb	Te	Au	Hg	Tl	Pb	Bi
Outokumpu		3	350000	25	300000	510	140	310000	290	0	0	0	120	9.1	22	50	0	0	0	0	0	0	1.1
		3	360000	25	300000	7	0	310000	310	7	0	0	53	8.8	25	51	0	0	0	0	0	0	0.4
		2	380000	0	300000	580	78	320000	380	4.5	0	0	77	24	0	86	0	0	0	300	0	0	1.0
		2	370000	6.5	300000	180	12	320000	320	3.8	0	0	71	5	0	80	0	0	0	200	0	0	0.6
Pumpkin Hollow	NCO8-39-1183	3	na	21.1	300000	0	0	304174	150	0	0	0	0	59	0	12	0	0	0	1025	0	1.4	1.1
	NCO8-39-1183	3	na	3.37	300000	5.6	0	294133	350	0	0	0	51	48	0	12	0	9.5	0	0	0.2	0	0
	NCO8-39-1183	3	na	8.18	300000	13	0	314273	1150	0	0	0	47	50	13	21	0	0	0	576	0	0	0
	NCO8-39-1183	3	na	7.81	300000	5.6	0	326766	970	0	0	0	43	55	14	16	0	9.1	0.22	0	0	0	0
	NCO8-39-1183	4	na	9.7	300000	14	17	309682	3223	0	0	0	51	44	0	8.3	0	0	0	385	0	1.9	0.9
	NCO8-39-1183	4	na	6.08	300000	10	0	308319	171	0	3.8	0	66	50	0	11	0	0	0	0	0	0	0.3
	NCO8-39-1183	4	na	6.46	300000	10	0	310396	435	0	0	0	47	65	13	7.9	0	0	0	3149	0.2	1.0	0.3
	NCO8-39-1183	8	na	6.70	300000	2.5	0	310089	433	0	0	0	0	67	0	13	0	0	0	805	0	0.8	0
	NC08-39-1269	58	na	13.8	300000	6.1	198	322186	280	0	0	0	0	99	0	13	0	8.9	0	0	0	2.4	0
	NC08-39-1269	58	na	9.5	300000	6.2	0	312660	333	0	0	0	128	98	0	11	0	0	0	0	0	6.0	0.2
	NCO8-39-1183	15	na	4.79	300000	12	0	327728	800	0	0	0	0	63	0	14	0	0	0	0	0	0.8	0
	NC08-49-1661	33	na	10.3	300000	15	101	292638	316	0	4.3	10	302	65	0	13	0	0	0	0	0	3.8	4.3
	NC08-49-1661	33	na	0	300000	4.1	18	314035	297	0	0	0	72	61	0	11	0	23	0.34	132	0	1.5	0.8
	NC08-49-1661	36	na	7.57	300000	0	0	326191	424	0	0	0	142	71	0	10	3.1	6.7	0.83	0	0	0	1.0
	NC08-49-1661	36	na	8.41	300000	6.7	0	298904	313	0	0	4.6	0	54	0	12	0	0	0	0	0.2	1.3	0
	NC08-49-1703	45	na	4.89	300000	0	0	316770	779	0	0	4.3	74	68	0	11	4.6	0	0	0	0	4.2	3.0
	NC08-49-1703	45	na	8.93	300000	1.8	0	314821	679	0	0	4.1	60	79	0	11	0	0	0	98	0	1.1	0.4
	NC08-49-1703	48	na	7.01	300000	2.1	0	317412	662	0	0	0	273	106	0	12	0	0	0	0	0.2	1.7	0.3
	NC08-49-1703	48	na	7.08	300000	0	0	308033	653	0	6.1	0	211	81	23	11	0	0	0	0	0	0.6	0
	NC08-49-1703)	48	na	8.12	300000	0	0	315249	1093	0	0	0	0	88	26	8.3	0	0	0.25	92	0	2.0	1.0
	NC08-20-1213	52	na	5.13	300000	0	8.8	300619	472	0	0	0	0	113	17	58	0	0	0	0	0	3.6	0.3
	NC08-20-1213	52	na	7.13	300000	2.3	0	321122	1060	0	0	5.8	0	103	0	63	2.5	8.6	0	0	0	2.1	0.6
	NC08-19-1531	21	na	6.08	300000	114	41	301999	497	0	0	0	98	95	0	25	0	0	0	0	3.3	12	1.3
	NC08-19-1531	21	na	3.34	300000	8.9	0	315434	703	0	0	0	99	105	0	26	0	0	0	0	0	1.7	0
	NC08-19-1531	21	na	7.75	300000	3.7	0	334286	638	0	4.0	4.3	106	96	0	22	0	0	0	0	0	0	0
	NC08-19-1531	25	na	7.08	300000	95	32	310697	502	0	0	0	0	107	16	33	0	0	0	0	0	2.4	1.5
	NC08-19-1531	25	na	13.6	300000	112	52	322850	821	0	0	0	0	112	0	24	0	0	0	0	0	0.0	0.4
	NC08-19-1531	28	na	6.67	300000	9.3	0	326132	413	0	0	0	48	117	0	19	0	0	0.27	0	0	0.7	0.4
	NC08-19-1531	28	na	5.10	300000	7.2	0	294739	529	0	0	0	133	102	0	18	0	6.8	0	0	0	1.0	0.7
	NC08-19-1531	28	na	8.12	300000	116	16	306071	535	0	3.5	0	129	105	0	24	0	9.1	0	0	0	0.8	0.4
	NC08-19-1531	31	na	8.45	300000	5.9	0	328102	732	0	0	6.8	0	112	0	16	0	0	0	0	0	0	0
	NC08-19-1531	31	na	9.9	300000	7.5	10	326032	1078	0	0	0	110	119	0	20	0	6.9	0	0	0	0.7	0.7
	NC08-19-1531	31	na	5.58	300000	4.7	0	326560	653	0	0	0	53	118	0	16	0	0	0.39	0	0	0	0.4

Table 4. Spot analyses of magnetite by LA-ICP-MS (values in ppm by weight).Differences between the core (cor), interior (in), outer (out), and rim portions of a few grains are indicated.

Locality	Sample #	Grain	Mg	Al	Si	S	Ti	V	Cr	Mn	Fe	Co	Ni	Cu	Zn	Ga	Ge	As	Se	Ag	Cd	In	Sb	Te	Au	Hg	Tl	Pb	Bi
Grasberg	Gras-1	1	820	2700	0	0	4100	1500	0	2000	700000	28	0	32	910	65	0	0	0	0	0	0	0	0	0	0	0	0	0
		1	1600	2400	0	0	3900	1500	116	1700	700000	34	0	36	640	83	0	0	0	0	0	0	0	0	0	0	0	0	0.56
		1	1900	2900	0	0	5700	1900	89	242	700000	3.9	0	31	250	75	0	0	0	0	25	0	0	0	0	0	0	11	1.1
		3	2500	2300	0	0	4400	2010	0	1400	700000	32	0		590	64	10	0	0	0	0	0	0	0	0	0	0	0	0
		3	460	2300	0	0	4400	2000	0	480	700000	13	0	180	530	59	0	0	0	0	0	0	0	11	1.2	0	0	0	0
Republic	OD-14895	2	76	0	0	0	0	0	0	955	700000	2.7	0	25	134	6.8	15	25	0	0	0	0	7.8	0	0	0	0	0	7.2
		2	1003	0	5600	0	0	31	0	1110	700000	3.4	12	53	48	20	0	0	0	0	0	0.99	5.3	0	0	0	0	0	2.0
		1	0	0	0	0	0	0	0	630	700000	1.1	3.8	2350	29	0	0	12	0	0	0	0.63	0	0	0	0	0	2.8	1.1
Pumpkin Hollow	NC08-49-1703	1	934	3779	0	0	152	66	0	282	700000	0	71	0	90	17	0	0	0	0	0	0	0	0	0	0	0	2.4	0
	NCO8-39-1183	1 rim	278	806	0	0	110	39	0	230	700000	5.4	0	0	0	9.7	0	0	0	0	0	0	0	0	0	0	0	0	0
	NCO8-39-1183	1 in	1457	3310	8538	0	206	47	0	269	700000	5.8	0	0	0	10	0	0	0	0	0	0	0	0	0	0	0	0	0
	NCO8-39-1183	1 out	1199	2336	6796	0	136	50	0	310	700000	9.8	0	0	0	12	0	0	0	0	0	0	0	0	0	0	0	1.1	0
	NCO8-39-1183	1 cor	3196	7449	17739	0	123	65	0	354	700000	12	0	514	79	11	0	13	0	0	0	0	0	0	0	0	0	8.3	1.8
	NCO8-39-1183	2 rim	37	500	0	0	0	49	0	160	700000	10	0	0	0	0	0	0	0	0	0	0	0	0	0	0	0	0	0
	NCO8-39-1183	2 in	1126	2980	7420	0	394	49	0	295	700000	8.0	0	0	0	10	0	0	0	0	0	0	0	0	0	0	0	0	0
	NCO8-39-1183	2 out	1660	4001	9598	0	257	34	0	337	700000	5.8	0	0	0	11	0	0	0	0	0	0.71	0	0	0	0	0	1.6	0
	NCO8-39-1183	2 cor	1516	3078	8687	0	197	23	0	323	700000	8.8	0	31	0	11	0	0	0	0	0	0	0	0	0	0	0	0	0
	NCO8-39-1183	2 rim	4145	10567	17244	0	95	76	0	356	700000	8.0	0	0	69	10	0	13	0	0	0	0	0	0	0	0	0	3.4	0
	NC08-20-1213	55	1228	5686	6252	0	308	243	0	314	700000	0	0	0	0	34	0	0	0	0	0	0	0	0	0	0	0	1.4	0
	NC08-20-1213	55	1735	9782	13048	0	952	223	0	377	700000	5.1	0	0	0	37	0	0	0	0	0	0	0	0	0	0	0	8.5	0
	NC08-20-1213	55	2215	11319	9808	682	542	266	46	371	700000	0	0	0	0	45	0	0	0	3.7	0	0	0	0	0	0	0	1.9	0
	NC08-19-1531	23	13739	17826	28096	0	849	102	0	211	700000	9.9	0	0	0	22	0	0	0	0	0	0	0	0	0	0	0	2.7	0
	NC08-19-1531	23	7097	12555	18867	0	946	303	0	203	700000	6.4	0	0	72	19	0	0	0	0	0	0	0	0	0	0	0	0	0
	NC08-19-1531	27	2590	12739	15618	0	557	54	0	154	700000	7.8	0	0	0	27	0	0	0	0	0	0	0	0	0	0	0	1.4	0.68
	NC08-19-1531	27	5592	17404	16922	0	824	101	0	194	700000	9.3	0	0	0	26	0	0	0	0	0	0	0	0	0	0	0	1.4	0
	NC08-19-1531	27	23717	22785	27946	1251	353	68	0	566	700000	9.9	0	0	0	12	15	0	0	0	0	0	0	0	0	0	0	1.3	0.92
	NC08-49-1703	43	35	254	0	0	69	70	0	235	700000	4.3	73	0	0	16	0	0	0	0	20	0	0	0	0	0	0	0	0
	NC08-49-1703	43	630	3576	0	0	291	112	0	244	700000	0	62	0	0	17	0	0	0	0	0	0	0	0	0	0	0	0	0
	NC08-49-1703	43	5310	12456	13322	753	1317	123	0	301	700000	3.29	130	26	0	21	0	11	0	0	0	0	8.3	0	0	0	0.81	3.4	0

APPENDIX (cont'd)

Table 5. Spot analyses of pyrite by LA-ICP-MS (values in ppm by weight).

Locality	Sample #	Grain	S	Mn	Fe	Co	Ni	Cu	Zn	Ga	Ge	As	Se	Ag	Cd	In	Sb	Te	Au	Hg	Tl	Pb	Bi
Bingham	OD-9927	1	520000	0	470000	7.1	51	6300	0	0	0	0	95	1.4	0	0	0.0	0	0	0	0	0	0
		1	520000	0	470000	18	16	8.7	0	0	0	0	0	0	0	0	0	0	0	0	0	0	0
		1	510000	0	470000	17	6.1	880	0	0	0	0	210	0	0	0	0	0	0	0	0	0	0.57
		2	530000	0	470000	3.7	3.3	18	1900	0	0	0	0	0	0	0	0	0	0	0	0	0	0
		2	510000	0	470000	1.2	0	39	0	0	0	0	0	0	0	0	0	0	0	0	0	0	0
		2	500000	0	470000	21	33	3100	0	0	0	0	98.4	0	0	0	0	0	0.21	0	0	11	1.6
		3	580000	0	470000	5	52	14000	0	0	0	0	250	7.3	0	0	0	0	0	0	0	13	1.5
		3	520000	0	470000	1.1	0	31	17	0	0	0	0	0	0	0	0	0	0	0	0	0	0
Chuqui	OD-47214	1	560000	0	470000	0	0	183	0	0	0	0	0	0	0	0	0	0	0	0	0	0	0.25
		1	630000	0	470000	0	0	1400	0	0	0	0	0	0	0	0	0	0	0	0	0	0	0
		2	480000	0	470000	0	0	570	0	0	0	42	0	4	0	0	0	0	0	0	0	0	0.67
		2	630000	0	470000	0	0	132	0	0	5.4	0	0	1.8	0	0	1.2	0	0	0	0	13	0.79
		3	540000	0	470000	0	0	170	0	0	0	0	0	0	0	0.36	0	0	0	0	0	0	0
Grasberg	Gras-1	2	610000	0	470000	790	76	0	67	0	0	0	180	0	0	0	0	0	0	0	0	4.9	3.4
		2	560000	0	470000	270	10	0	430	0	0	0	240	0	0	1.4	0	0	0	0	0	5.4	1.8
Cananea-Capote	OD-20003	1	590000	0	470000	0	0	47	0	0	0	0	0	2.5	0	0	0	0	0	0	0	0	0
		1	590000	0	470000	0	0	31	0	0	0	0	0	1.2	0	0	0	0	0	0	0	0	0
		1	590000	0	470000	0	0	24	0	0	0	0	0	0	0	0	0	0	0	0	0	0	0
		2	540000	0	470000	0	0	0	0	0	0	23	0	5.7	0	0	0	0	0	0	0	0	0
		2	590000	0	470000	2.6	0	36	0	0	0	0	0	0	0	0	0	0	0	0	0	0	0
		4	560000	0	470000	0	0	35	0	0	0	0	0	0	0	0	0	0	0	0	0	0	0
		4	540000	0	470000	0	0	56	0	0	0	0	0	0	0	0	0	0	0	0	0	0	0
		4	560000	0	470000	0	0	36	0	0	0	0	0	5.9	0	0	0	0	0	0	0	0	0
Republic	OD-14895	7	604000	0	470000	110	42	0	0	0	0	15	61	0	0	0	0	0	0	0	0	5	9.8
		7	554000	0	470000	14	90	0	19	0	0	13	64	1.4	0	0	0	0	0	0	0	6.7	9.8
		7	543000	0	470000	81	91	43	0	0	0	47	0	15	0	0	2.0	0	0	0	0.72	41	29
		7	602000	0	470000	1.6	193	9.2	18	0	0	39	101	0	0	0	0	0	0	0	0	0	1.8
		7	645000	0	470000	28	335	82	0	0	0	33	73	0	0	0	0	9.3	0	0	0	0	0.38
		7	590000	0	470000	194	155	0	0	0	0	52	120	0	0	0	0	0	0	0	0	4.9	13
Pumpkin Hollow	NCO8-39-1183	5	na	12	470000	0	0	0	0	0	0	0	60.1	10	0	0	2.0	0	0	0	0	0	0
	NCO8-39-1183	5	na	12	470000	9.0	19	50.6	0	0	0	0.0	62.4	1.4	0	0.37	0.0	0	0	272	0	0	0
	NCO8-39-1183	7	na	20	470000	5.3	67	2184	462	0	0	7.8	147	43	0	1.1	4.6	0	0	315	0	1.6	0
	NCO8-39-1183	7	na	14	470000	0.0	14	1328	603	0	0	0	0.0	30	0	2.2	3.7	0	0	163	0	2.2	0
	NCO8-39-1183	7	na	27	470000	2.7	22	1583	1733	0	0	0	68.4	47	0	13	1.7	0	0	459	0	8.1	0
	NCO8-39-1183	9	na	17	470000	2.3	12	899	153	0	0	0	92.5	23	0	1.4	2.0	0	0	0	0	5.4	0
	NCO8-39-1183	9	na	17	470000	0	29	1472	425	0	0	0	55.4	15	0	3.8	2.2	0	0	0	0	5.8	0
	NCO8-39-1183	9	na	18	470000	0	0	1928	633	0	0	0	40.2	21	0	6.5	0	0	0	0	0	7.4	0.23
	NCO8-39-1183	12	na	12	470000	848	601	0.0	0	0	0	0	40.4	35	0	0	0	0	0	275	0	3.4	0.24
	NCO8-39-1183	12	na	9.1	470000	858	597	0	0	0	0	0	57.8	0.0	0	0	0	0	0	0	0	0.93	0
	NCO8-39-1183	13	na	14	470000	474	429	0	0	0	0	0	0	4.8	0	0	0	0	0	0	0	1.2	0.47
	NCO8-39-1183	13	na	12	470000	607	390	0	0	0	0	0	43.0	6	0	0	0	0	0	768	0	0.80	2.0
	NCO8-39-1183	14	na	22	470000	946	470	0	0	0	0	0	0.0	2257	0	0	0	0	0	1399	0	1.0	0
	NCO8-39-1183	16	na	11	470000	875	522	0	0	0	0	0	0.0	63	0	0	0	0	0	0	0	3.4	0.34
	NCO8-39-1183	16	na	10	470000	1212	740	0	0	0	0	0	132	2.3	0	0	0	0	0	0	0	1.9	0
	NCO8-39-1183	16	na	8.3	470000	503	345	0	0	0	0	0	88.7	0	0	0	0	0	0	0	0	0	0
	NCO8-39-1183	17	na	15	470000	932	376	0	0	0	0	0	55.3	17	0	0	0	0	0	0	0	2.2	0
	NCO8-39-1183	17	na	14	470000	958	528	0	0	0	0	0	112	34	0	0	0	18	0	0	0	2.1	0
	NCO8-39-1183	17	na	15	470000	959	492	0	0	0	0	0	70.5	3.9	15	0	0	0	0	0	0	1.7	1.3
	NCO8-39-1183	18	na	6.9	470000	437	264	0	0	0	0	0	47.7	5.5	0	0	0	0	0	0	0	0	0
	NC08-39-1269	56	na	11	470000	8.9	15	68.2	0	0	0	10	156	8.3	0	0	28	0	0	0	0	0.909	0

APPENDIX (cont'd)

Table 5. Spot analyses of pyrite by LA-ICP-MS, **continued**.

Locality	Sample #	Grain	S	Mn	Fe	Co	Ni	Cu	Zn	Ga	Ge	As	Se	Ag	Cd	In	Sb	Te	Au	Hg	Tl	Pb	Bi
Pumpkin Hollow	NC08-39-1269	56	na	10	470000	10	9.9	0	0	0	0	8.9	186	9.4	0	0	8.8	0	0	0	0	1.7	0
	NC08-39-1269	56	na	12	470000	8.2	0	0	0	0	0	6.6	71.9	0	0	0	4.6	0	0	0	0	0.87	0.25
	NC08-39-1269	57	na	23	470000	691	1072	0	0	0	0	7.8	99.6	1.3	0	0	14	0	0	0	0	1.1	0
	NC08-39-1269	57	na	12	470000	330	186	0	0	0	0	4.1	131	0	0	0	5.6	0	0	0	0	0	0
	NC08-49-1661	32	na	13	470000	853	9063	140	100	0	0	91	108	26	0	1.9	4.3	0	0	0	0	31	4.5
	NC08-49-1661	34	na	34	470000	346	4697	112	217	0	0	4281	160	9.0	0	10	20	0	0	0	1.9	13	3.0
	NC08-49-1703	36	na	12	470000	528	140	0	0	0	0	421	117	0	0	0	0	0	0	0	0	0.46	1.5
	NC08-49-1703	36	na	11	470000	560	252	0	0	0	0	73	118	0	0	0	0	0	0	0	0	0.66	0
	NC08-49-1703	36	na	12	470000	399	293	0	0	0	0	59	108	0	0	0	8.3	0	0	0	0	0	0
	NC08-49-1703	38	na	14	470000	7752	50	0	0	0	0	263	113	0	0	0	0	0	0	0	0	1.9	11
	NC08-49-1703	38	na	12	470000	4020	349	0	0	0	0	122	78	3.4	0	0	2.0	0	0	0	0	11	18
	NC08-49-1703	38	na	11	470000	2420	100	0	0	0	0	34	71	0	0	0	0	0	0	0	0	0	0
	NC08-49-1703	39	na	12	470000	397	3328	0	0	0	0	0	202	0	0	0	0	0	0	0	0	0.99	1.5
	NC08-49-1703	39	na	22	470000	274	2772	0.0	0	0	0	4.8	47.8	1.8	0	0	1.8	12	0	0	0	3.8	4.3
	NC08-49-1703	40	na	13	470000	1561	229	0.0	0	0	0	150	0.0	0	0	0	0	0	0	0	0.30	0.97	2.3
	NC08-49-1703	40	na	14	470000	620	207	0.0	0	0	0	57	0.0	0	0	0	0	0	0	0	0	0.51	4.1
	NC08-49-1703	40	na	7.6	470000	286	94	0	0	0	0	74	58	0	0	0	0	0	0	0	0	0	0
	NC08-49-1703	42	na	14	470000	378	274	0	0	0	0	270	125	0	0	0	0	0	0	0	0	0.47	1.4
	NC08-49-1703	42	na	22	470000	503	170	0	0	0	0	47	75	0	0	0	0	0	0	0	0	0	2.8
	NC08-49-1703	44	na	17	470000	9.3	144	0	0	0	0	158	53	0	0	0	4.8	0	0	0	0	0	0
	NC08-49-1703	44	na	23	470000	11	133	0	0	0	0	56	62	3.0	0	0	3.3	0	0	0	0	0	0
	NC08-49-1703	46	na	10	470000	3716	81	0.0	0	0	0	630	0	0	0	0	0	0	0	0	0	0	0.53
	NC08-49-1703	56	na	8.6	470000	1040	120	0	0	0	0	101	46	0	0	0	0	0	0	0	0	0	0.39
	NC08-49-1703	47	na	62	470000	47	214	0	0	3.0	0	13	144	0	0	0	33	0	0	175	0	3.3	0.52
	NC08-49-1703	47	na	17	470000	34	165	0	0	0	0	0	122	0	0	0	34	0	0	0	0	1.1	0
	NC08-49-1703	47	na	18	470000	58	449	0	0	0	0	106	48	0	0	0	8.0	0	0	0	0	0	0
	NC08-49-1703	47	na	11	470000	4.5	75	1849	529	0	0	0	106	19	0	18	16	0	0	0	0	1.4	0
	NC08-20-1213	49	na	7.1	470000	0	35	0	0	0	0	0	0	2.7	0	0	0	0	0	0	0	1.0	0
	NC08-20-1213	49	na	11	470000	0	40	58	0	0	0	51	96	14	0	0	9.0	0	0	0	0	0.68	0
	NC08-20-1213	49	na	10	470000	2.1	51	90	0	0	0	2819	60	38	0	0.85	91	0	0.22	0	0	1.3	0
	NC08-20-1213	49	na	12	470000	0	28	56	0	0	0	574	90	11	0	0	35	0	0	0	0	0.61	0
	NC08-20-1213	51	na	14	470000	129	1012	0	0	0	0	7.94	117	11	0	1.0	0	0	0	0	0	6.9	1.4
	NC08-20-1213	51	na	12	470000	170	1161	0	0	0	0	14	145	1.5	0	0	0	0	0	0	0	1.9	0.33
	NC08-20-1213	51	na	23	470000	240	1041	0	0	0	0	11	85	0	0	0	0	0	0	0	0	2.9	0
	NC08-20-1213	53	na	9.2	470000	271	649	0	0	0	0	0	47	0	0	0	0	0	0	0	0	0	0
	NC08-20-1213	53	na	11	470000	270	936	0	0	0	0	0	124	0	0	0	0	0	0	0	0	0	0
	NC08-19-1531	19	na	12	470000	608	269	0	0	0	0	0	0	0	0	0	1.8	0	0	0	0	0	0.0
	NC08-19-1531	19	na	10	470000	758	384	0	0	0	0	0	0	2.1	0	0	1.9	0	0	0	0	0.85	0.27
	NC08-19-1531	19	na	9.0	470000	25	14	0	0	0	0	0	0	0	0	0	0	0	0	0	0	0	0
	NC08-19-1531	24	na	7.0	470000	763	361	0	0	0	0	0	69	0	0	0	2.8	0	0	0	0.41	3.4	0.88
	NC08-19-1531	24	na	8.1	470000	550	295	0	0	0	0	0	73	0	0	0	0	0	0	0	0	0.46	0.25
	NC08-19-1531	24	na	8.7	470000	684	264	857	0	0	0	0	47	6.2	0	0	6.2	0	0	0	0.39	4.0	1.9
	NC08-19-1531	30	na	12	470000	508	198	0	0	0	0	0	82	0	0	0	61	0	0	0	1.5	0	0
	NC08-19-1531	30	na	10	470000	601	292	0	0	0	0	0	45	0	0	0	137	0	0	0	1.5	0	0.60
	NC08-19-1531	30	na	12	470000	719	365	0	0	0	0	0	45	0	0	0	52	0	0	0	1.2	0	0.50
	NC08-19-1531	30	na	12	470000	545	257	0	0	0	0	5.2	54	2.5	0	0	82	0	0	0	4.7	1.2	0.37
	NC08-19-1531	19	na	12	470000	947	428	0	0	0	0	0	0	0	0	0	2.6	0	0	0	0	2.3	1.3
	NC08-19-1531	19	na	10	470000	985	443	0	0	0	0	0	90	0	0	0	2.0	0	0	0	0	2.1	0.42
	NC08-19-1531	19	na	11	470000	712	343	0	0	0	0	0.0	41	0	0	0	2.3	0	0	0	0	0	0

APPENDIX (cont'd)

Table 6. Spot analyses of pyrrhotite, bornite, chaclcocite, tennantite, covellite, enargite, and sphalerite by LA-ICP-MS (values in ppm by weight). Values below the detection limit are listed as zero; na = not analyzed.

Mineral	Locality	Sample #	Grain	S	Mn	Fe	Co	Ni	Cu	Zn	Ga	Ge	As	Se	Ag	Cd	In	Sb	Te	Au	Hg	Tl	Pb	Bi
Pyrrhotite	Pumpkin Hollow	NCO8-39-1183	11	na	20	600000	675	970	44.5	5375	2.6	0	0	96	12	22	9.3	0	0	0	0	0	4.4	1.1
			11	na	17	600000	339	367	0	0	0	0	0	73	8.3	0	0	1.6	0	0	980	0	1.3	0.49
			11	na	17	600000	445	414	0	0	4	0	10	0	9.0	0	0	0	12	0	455	0	3.9	0.59
			18	na	17	600000	706	436	0	0	0	6.1	0	178	12	0	0	0	11	0.34	95	0	0.99	0.00
			18	na	12	600000	572	237	0	0	0	0	0	89	17	0	0	0	0	0	0	0	0.63	2.8
		NC08-19-1531	20	na	12	600000	527	219	0	0	0	5.5	0	67	1.6	0	0	0	0	0	0	0.25	1.0	0.56
			20	na	12	600000	586	277	0	0	0	0	0	0	1.2	0	0	0	0	0	0	0	0	0.00
			20	na	8.5	600000	484	244	0	27	0	0	0	0	0	25	0	0	0	0	125	0	0.0	0.26
			22	na	6.7	600000	499	139	0	0	0	0	0	71	1.7	0	0	0	15	0.43	0	0	1.2	0.00
			22	na	11	600000	547	236	0	0	2	0	0	196	0	0	0	0	9.7	0	0	0	0	0.00
			26	na	16	600000	539	267	0	0	0	0	0	99	0	0	0	0	0	0	0	0	0.73	0.51
			26	na	18	600000	571	245	0	0	0	0	0	65	0	0	0	0	0	0	0	0	2.6	1.1
			26	na	18	600000	696	392	0	0	0	0	0	105	5.6	14	0	2.4	0	0	0	0	0	1.5
			29	na	17	600000	476	149	0	0	0	0	8.4	0	2.5	44	0	0	0	0.50	0	0	0	0.72
			37	na	12	600000	399	160	0	0	0	0	0	110	0	16	0.44	0	0	0	0	0	0	0.00
		NC08-49-1661	41	na	50	600000	808	4614	0	0	0	0	0	194	0	0	0	1.6	0	0.45	0	0	2.1	2.4
			41	na	13	600000	690	4534	0	25	0	0	0	131	2.3	0	0	0	0	0	0	0	7.9	5.1
			41	na	13	600000	760	4633	0	0	0	3.7	0	429	1.9	0	0.38	0	9.7	0	0	0	5.1	3.2
Pyrrhotite	Outokumpu	OD-31756	3	370000	5.8	600000	710	770	91	0	0	0	0	0	1.1	33	0	0	0	0.19	0	0	0	1.0
			3	380000	9.6	600000	480	700	0	0	0	0	8.7	0	0	0	0.56	0	0	0.25	0	0	8.5	3.8
			1	350000	0	600000	460	730	0	0	0	0	0	73.3	0	0	0	0	0	0.26	125	0	0	0
			1	370000	0	600000	650	710	0	0	0	0	0	120	1.8	0	0	0	0	0	0	0	0	0
			2	403000	4.2	600000	590	810	0	22	0	7	12	90	0	23	0	0	0	0	0	0	0	0
			2	403000	0	600000	610	850	0	0	0	0	0	0	0	0	0	0	0	0	0	0	2.6	0.6
Bornite	Cananea Colorada	OD-20003	1	270000	0	110000	0	0	510000	33	0	0	0	170	69	0	0	0	0	0.63	0	0	15	430
			1	280000	0	110000	0	0	540000	0	0	0	0	170	102	0	0.69	0	7.4	9.3	0	0	3.9	410
			1	270000	6.6	110000	0	0	510000	27	0	0	0	110	92	36	0.53	0	0	1.1	0	0.44	3.6	470
			2	270000	13	110000	0	0	470000	20	0	0	0	96	68	0	1.3	0	0	2	290	0.72	31	480
			2	260000	9.3	110000	0	0	460000	38	0	0	0	56	82	0	0	0	8.4	0.18	0	0	9.7	500
Chalcocite	Bingham	OD-9927	1	290000	0	2200	6.7	0	790000	14	0	0	145	69	130	0	0	0	16	0.48	0	6	0	4.6
			1	290000	0	3400	2.1	0	790000	22	0	0	285	190	140	0	0.96	0	12	1.2	0	5.7	24	53
			2	300000	0	3900	8	0	790000	15	0	4.6	23	260	120	0	0.3	0	0	0	0	2.1	4.4	3.2
			2	280000	0	8300	17	7	790000	21	0	0	7.4	190	85	0	0	0	0	0	0	1.7	4.4	12
			3	270000	0	5800	7	0	790000	34	0	0	170	180	130	45	0	2.3	0	0.82	0	6.6	9.9	73
			3	290000	0	13000	0	0	790000	79	0	0	27	220	100	0	0	0	16	0	0	5.1	5	250
Chalcocite	Cananea Colorada	OD-20003	1	350000	0	3400	0	0	790000	230	0	0	0	200	250	0	2.9	1.4	0	2.7	0	0.17	28	130
			1	370000	0	67000	0	0	790000	160	0	0	0	250	140	0	0.36	0	13	1.2	0	0.17	0	550
			2	340000	0	4500	1.1	0	790000	8.7	0	0	0	0	220	0	0	0	0	2.3	0	0	6.9	401
			2	380000	140	10200	3.8	0	790000	760	0	5.4	0	91	440	27	7.4	0	44	10	0	0.64	230	280
Tennantite	Chuqui	OD-47214	1	580000	16	226	0	0	500000	550	0	1500	280000	60	140	0	0	24000	190	0	0	0.99	100	46
			1	460000	0	363	1.9	0	500000	207	9.3	510	160000	0	790	110	2.2	4020	155	1.7	240	2.2	680	150
			2	580000	23	0	0	0	500000	137	0	460	290000	0	140	37	0.52	8800	220	0	0	0.24	280	49
			2	580000	0	250	0	0	500000	84	0	420	280000	0	6.6	0	0	26000	20	0	0	0	2.1	3.8
			3	520000	0	231	0	0	500000	174	0	513	230000	92	120	120	0.4	9000	19	0.29	0	0.46	96	24

APPENDIX (cont'd)

Table 6. Spot analyses of pyrrhotite, bornite, chaclcocite, tennantite, covellite, enargite, and sphalerite by LA-ICP-MS, **continued**.

Mineral	Locality	Sample #	Grain	S	Mn	Fe	Co	Ni	Cu	Zn	Ga	Ge	As	Se	Ag	Cd	In	Sb	Te	Au	Hg	Tl	Pb	Bi
Covellite	Cananea Colorada	OD-20003	1	550000	510	18000	1.2	0	660000	560	0	0	12.8	260	560	44	5.7	0	0	31	0	16	190	310
			1	550000	160	15000	0	0	660000	110	0	0	0	250	680	19	4.9	0.97	0	36	0	24	130	210
			2	520000	13	5100	0.86	0	660000	43.1	0	0	6.1	210	510	0	5.9	1.5	0	32	0	24	93	200
			2	420000	170	84000	2.1	0	660000	1500	0	0	5.8	180	1400	76	13	1.1	0	41	0	3.9	290	870
Enargite	Cananea Capote	OD-20021	1	470000	0	3000	3.3	2.6	480000	15000	0	0	290000	0	2400	380	210	4.2	4.9	2.8	550	190	10100	580
			1	420000	0	3000	1.4	0	480000	102000	0	0	230000	0	230	600	360	97	0	0.62	700	14	600	120
			2	340000	0	5000	3.6	5.9	480000	72000	4.4	43	170000	0	750	290	270	1.4	11	2.2	1300	76	3200	330
			2	470000	21	6400	1500	4.8	480000	140000	0	840	220000	0	690	200	1200	71	3.6	1.3	240	58	7200	5000
Sphalerite	Republic	OD-14895	1	368000	730	37100	332	0	31200	640000	3.4	0	4.1	39	19	4090	107	1.9	0	0	0	0	0	0.78
			1	366000	2000	34500	294	0	29800	640000	3.0	0	4.2	59	16	3650	106	0.9	0	0	0	0	4.3	3.4
			2	356000	1300	29400	242	0	20500	640000	2.8	0	0	77	15	3670	108	1.8	0	0	0	0	12	9.0
			2	368000	2900	37500	269	0	33900	640000	3.0	0	0	61	23	3650	91	0	0	0	0	0	0	0
			3	373000	5100	80100	209	0	71	640000	4.0	0	0	65	1.1	3650	94	0	0	0	0	0	0	0
			3	363000	3800	28600	232	0	15600	640000	4.1	0	0	57	7.2	3250	96	0	0	0	0	0	0	0
Sphalerite	Outokumpu	OD-31756	2	370000	13000	83000	3300	0	190	640000	5.3	0	0	71	3.5	2897	367	0	0	0	0	0	0	8.5
			3	430000	16000	16000	4200	0	83000	640000	0	0	0	120	9.8	2271	218	0	0	0	0	0	14.1	9.4

Table 7. Detection limits for spot analyses of minerals by LA-ICP-MS.

	Mg	Al	Si	S	Ti	V	Cr	Mn	Fe	Co	Ni	Cu	Zn	Ga	Ge	As	Se	Ag	Cd	In	Sb	Te	Au	Hg	Tl	Pb	Bi
Chalcopyrite				12400		8.4	28	5.1	198	1	3.4	8.2	11	2.8	4.1	7.3	44	1.1	20	0.30	1.3	8.0	0.20	151	0.29	3.1	0.27
Chalcopyrite[1]						4.3	9.1	2.8	<300	1.6	5.9	<10	<10	1.6	3.5	3.8	39	<2	13	<1	1.5	6.6	0.21	87	0.22	0.40	0.21
Pyrite				3920		4.7	27	5.5	210	1.0	3.0	6.3	14	3.5	5.2	12	59	1.1	23	0.29	1.2	8.5	0.19	151	0.16	2.6	0.21
Pyrrhotite				594		3.7	12	3.8	73	1.3	2.9	9.0	12	1.6	5.8	3.0	70	0.91	16	0.26	1.5	13	0.09	102	0.25	2.4	0.48
Bornite				16600		10	32	5.3	141	0.96	3.1	8.2	12	3.0	3.3	6.6	39	1.1	20	0.27	1.2	5.9	0.15	174	0.39	2.5	0.27
Chalcocite				4250		5.0	26	10	125	1.0	4	9.8	8.3	2.1	4.4	3.7	44	1.7	27	0.28	1.2	7.0	0.38	224	0.16	2.6	0.27
Covellite				1670		6.1	35	4.8	79	0.81	2.3	14	6.4	3.8	7.1	3.7	79	0.54	18	0.28	0.59	13	0.19	93	~0.3	2.8	0.16
Tennantite				3590		3.9	19	6.2	97	1.7	4.8	5.7	5.2	2.7	7.2	17	58	0.97	13	0.29	0.79	7.2	0.14	173	0.15	1.4	0.62
Enargite				5640		1.8	14	3.1	91	0.87	2.5	12	6.6	1.9	6.0	11	47	1.7	25	0.30	1.3	3.1	0.16	59	0.13	1.9	~0.5
Sphalerite				2170		4.5	22	3.8	95	36	6.6	5.4	9.5	2.5	3.3	3.9	13	0.5	30	0.16	0.69	6.1	0.19	262	0.32	2.7	0.15
Magnetite	7.3	388	4710	440	77	11	76	12	na	2.2	9.7	23	45	6.0	7.8	15	15	2.9	24	0.57	3.7	8.2	0.74		0.72	6.0	0.40
Magnetite[2]	<35	<254	5359	577	58	<23	32	<150	na	3.3	29	14	57	4.7	7.6	10	20	3.3	14	0.68	3.7	9.4	0.52		0.61	1.0	0.65

[1]Detection limits for Pumpkin Hollow chalcopyrite, pyrite, and pyrrhotite analyses.
[2]Detection limits for Pumpkin Hollow magnetite analyses.
Blanks signify that no analyses were done for that element in that mineral; na = not applicable, because Fe was fixed at a specified value.